Detection and measurements of high pressure VLE and LLE - PvT data of binary mixtures through the vibrating tube densitometer technique.

M. Bárcenas Castañeda, C. Bouchot † *and L. A. Galicia Luna*
Instituto Politécnico Nacional, ESIQIE,
Laboratorio de Termodinámica,
Edif Z6 1ER *Piso,UPALM Zacatenco, 07738 Lindavista,*
México D.F., México.
† *Corresponding author*

Prepared for Presentation at the AIChE Annual Meeting, 2004,
Session 156 – Thermodynamic Properties and Phase Behavior I.
Unpublished.

Abstract

In this work we analyze the feasibility of detecting equilibrium states and measuring, simultaneously, saturated liquid densities and equilibrium pressures at fixed temperature, of "Type V" binary mixtures in state regions where both VLE and LLE are present. The employed technique is the Synthetic Indirect PvT Method through a single vibrating tube densitometer setup. The detection of phase equilibrium is performed by analyzing the topology of near continuous isothermal data acquisitions in the vicinity of the discontinuous phase transition at a saturation point. Close to the estimated equilibrium pressure, a flow rate of about 0.0002 MPa/s is set within the measuring instrument preserving the temperature stability, and the periods of vibration of the densitometer are sampled and registered every 3s. The collected data are analyzed by means of mathematical interpolations, and the data corresponding to the location of a change in the slope or in the curvature of the isothermal behavior is pointed out. We present examples of the topologies and data analysis obtained for synthetic mixtures of Ethane + n-Propan-ol at different temperatures in the region where they present liquid-liquid in-miscibility encompassing LLE and VLE at near critical conditions. The equilibrium data are discussed and compared with those available in the literature.

1 Introduction

Apart of the industrial interest that presents the study of the high pressure equilibrium behavior of solvent + co-solvent systems such as Ethane + Alcohol for the extraction of species from natural products cores, the ways these systems can be studied experimentally is also a very relevant issue. Some of these mixtures present rather complex phase behavior as a function of temperature and composition (see Lam et al. (1990) and Brunner (1985)) including liquid – liquid in-miscibility. Along with the equilibrium behavior, the coexisting phase densities are usefull for modeling and process design purpose as they provide a complete knowledge of the behavior of fluids at saturation.

High pressure Liquid – liquid equilibrium are quite difficult to study using the ordinary static – analytic methods because of the difficulties in sampling the liquid phases, particularly when

encountered near a critical point or critical end – point where their densities are similar. This work is some continuation of previous works of Bouchot and Richon (1998a,b) where it was shown that simultaneous pvT and VLE data of refrigerant mixtures could be measured by means of a single vibrating tube densitometer setup. In this presentation it is shown that a similar setup can be used to obtain simultaneously the densities and saturation pressures of synthetic mixtures of Ethane + n-Propan-ol at different temperatures in the regions where transitions between two liquid phases take place. The studied mixture pertains to the Type V phase diagram and is historically the first mixture of this kind ever encountered, see Sengers (2002).

In a first section the experimental setup used in this study is briefly described. In the second section the LLE detection procedure for binary mixtures of Ethane + n-Propan-ol at four different temperatures and five compositions are presented. First the detection procedure and the analytical access to the saturation densities are presented. Then the differences in the topology of the isotherms as a function of the type of transition are discussed and qualitatively compared with the data of Kodama et al. (2001).

2 Experimental setup

The vibrating tube technique for density measurements is widely used and discussed in the literature, for instance in Lagourette et al. (1992), Holcomb and Outcalt (1998) and references cited therein. In this study we use the Anton-Paar® DMA 512-P external cell calibrated with pure HPLC analysis grade degassed water and the vacuum reference point. Details about the calibration method can be found in Bouchot and Richon (2001) for the DMA 512 cell.

The current setup is that described in De la Cruz de Dios et al. (2003). The Loading and pressurizing procedures allow the best possible stability of the state variables at any condition. A piston actuated variable volume cell is used for mixture preparation by successive weightings (see Galicia Luna et al. (1994)). Weightings are performed on a modified Sartorius® LC1201S analytical balance with an accuracy of ±0.0002 g. The absolute uncertainty due to successive mass measurements and weightings irreproducibility) in compositions is about $\pm 5 \times 10^{-5}$ in mole fraction.

The DMA 512-P cell temperature is regulated and the rest of the experimental setup is maintained at controlled room temperature. A temperature stability of ±0.002 K is obtained during several minutes at any temperature in the working range. The temperature measurements are performed by means of a pt–100 resistance probe and an ASL® F250 thermometer with a total accuracy of ±0.02 K, between 263 K and 423 K.

The pressure is measured by means of a Druck®-PMP 4060 transducer, with a scale of 138 bar. This transducer is calibrated against a Desgranges & Huot® dead weight gauge (5304 S2, ± 0.005 % F.S. precision up to 1380 bar). The mass to pressure conversion coefficient of the gauge is corrected for the local gravity (Mexico City). The measured pressures have a standard deviation of ±0.013 bar from 1 to 140 bar.

An electronic data acquisition (see De la Cruz de Dios et al. (2003)) provides records of data points consisting in the temperature T, pressure p and τ (the period of the vibrating tube densitometer) recorded every 3 s. Measurements of τ(T, p) are performed so that, at stable T and p, the fluctuations are within $\pm 2 \times 10^{-6}$ and $\pm 5 \times 10^{-6}$ ms in approximately 2 s. This corresponds to absolute experimental fluctuations of less than $\pm 1 \times 10^{-4}$ kg m^{-3} in density. It is necessary to use quasi-static – static measurement procedures to reach this stability in the state variable. However, by means of a sufficiently low flow rate during quasi-static decompressions as described in Bouchot

and Richon (1998a), the measurements stability commented in De la Cruz de Dios et al. (2003) can be preserved.

3 LLE of the *Ethane+n-Propan-ol* mixture

In this work, the equilibrium data and near saturation p, τ , T behavior (similar to the p, ρ, T behavior, before the conversion of vibration periods into densities) for 5 mixtures of Ethane + n-Propan-ol at 4 different temperatures: 314.15 K, 315 K, 317 K and 320 K are presented. The compositions of the mixtures are x_{C2}=0.7187(5), 0.8302(9), 0.8546(9), 0.8741(0) and 0.9053(0) in mole fraction. According to Lam et al. (1990), Brunner (1985) and Kodama et al. (2001), the previous conditions correspond to mixtures that can present four types of phase transitions: heavy liquid (alcohol rich) - light liquid (Ethane rich); (L_H-L_L), light liquid - heavy liquid; (L_L-L_H), light liquid - gas; (L_L-G) and heavy liquid - gas; (L_H-G), at these temperatures above the critical point of Ethane.

The pure components used in this work are a scientific grade 99.999 % Ethane from Air Products Inc.-Infra S.A. and a dry 99.9 % pure n-Propan-ol from Aldrich Mexico S.A. Both fluids were used without further purification and n-Propan-ol was carefully degassed by partial evaporation under vacuum before use.

3.1 Detection of phase equilibrium

The saturation pressure at the beginning of the experiments was evaluated at each composition and temperature by means of an analysis of the data of Kodama et al. (2001). The procedure used to determine experimentally the location of a saturation point consists in a quasi – static decompression of the homogeneous fluid mixture from an initial pressure fixed between 65 and 75 bar for the studied system depending on the composition and temperature. The mixture is previously loaded an homogenized under pressure (about 130 bar in this case) within the whole measurement circuit. The temperature of the connecting tubing of the experimental setup is maintained at ambient temperature, always cooler than the regulated densitometer, to avoid any flash outside the vibrating tube. This procedure works for Type V mixture while, at a given composition, the saturation pressure of the fluid increases with temperature. This is the case for the Ethane + n-Propan-ol mixture up to about 403 K according to the data of Brunner (1985).

From the initial fixed pressure, a continuous flow through the measurement circuit is established at about 0.002 bar/s by means of a leaking through the relief valves of the circuit downstream from the vibrating tube. This low flow rate allows to maintain a stationary circulation of the fluid that preserves a quasi – static state and the thermodynamic equilibrium of the system at each recorded pressure. The flow rate was established on the base of the observation of the simultaneous stability of the vibrating period within its usual fluctuations (about $2 \times 10^{-6} ms$) while decreasing the pressure, and of the temperature with fluctuations within the range defined by the regulating device (about 0.002 K). The instant when the saturation is reached exactly within the vibrating tube can be captured visually, with the help of the automatic data acquisition. This is usually revealed by the observation of a change in the topology of the actual isotherm in the $p - \tau$ plane. Based on previous experiments on L-V transitions with this technique it was expected that, at a composition and temperature corresponding to a L – L transition, a breakpoint could be observed the same way as in the case of a L – V transition. It was also expected that the phenomenon would be less pronounced in the latter case. In a L – V transition, the detection phenomenon is observed

when a vapor bubble appears within the liquid phase and moves with high mobility throughout the vibrating tube impulsing a highly noticeable perturbation in its vibrating behavior. In the case of the L_H-L_L transition, the change in density within the tube when the first drop of light liquid is formed within the heavy phase should be drastically lower. Due to the almost capillary conditions of the fluid flow, such a drop should move slowly throughout the vibrating tube resulting in a less violent perturbation of the mechanical vibration.

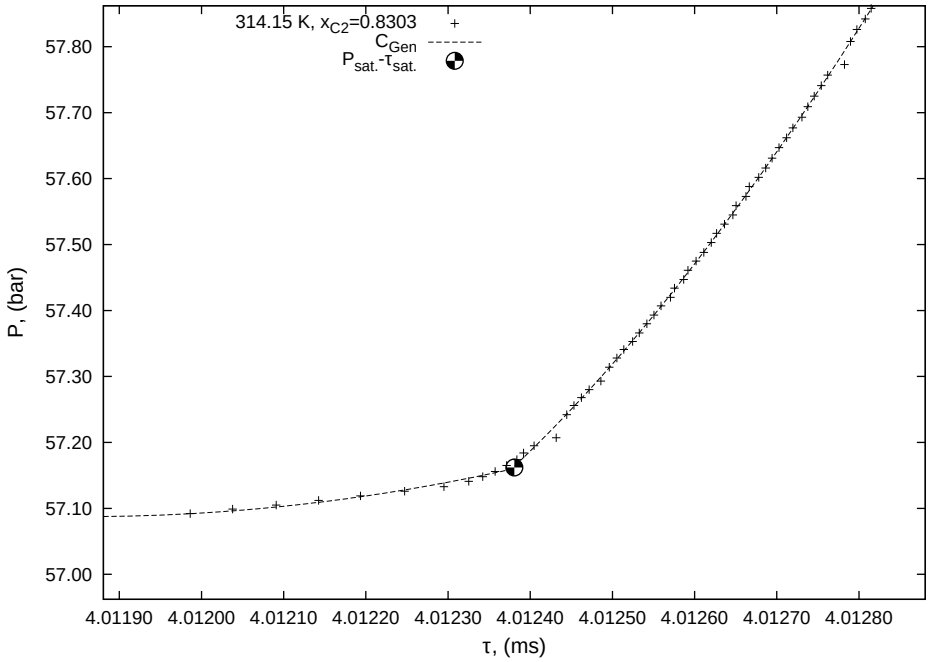

Figure 1: Detection of a L_H-L_L transition, x_{C2} =0.8303, 314.15 K

With this methodology, slow L_H-L_L transitions as shown in figure 1 in the p – τ plane could be observed. At x_{C2} =0.8303 the topology near the break point is really very similar to what occurs in a typical L – V or L – G transition as shown in figure 2. The difference between the two types of transition is that the slope of the data collected at the very beginning of the inhomogeneous region is smoother during the L – L transition than during the L – V one. When studying the system at a composition that would present a transition from a light liquid phase to a heavy one the behavior as shown in figure 3 is observed.

This L_L - L_H transition is detected in the same direction as the L_H - L_L, i.e. the density decreases when the system becomes inhomogeneous. This shows that the negative density difference between the two liquids is not the principal cause of the behavior of the transition within the tube. The fact that the density keeps lowering while denser drops are formed within the vibrating tube can be understood when considering the p– ρ– x behavior of such a system within the instrument.

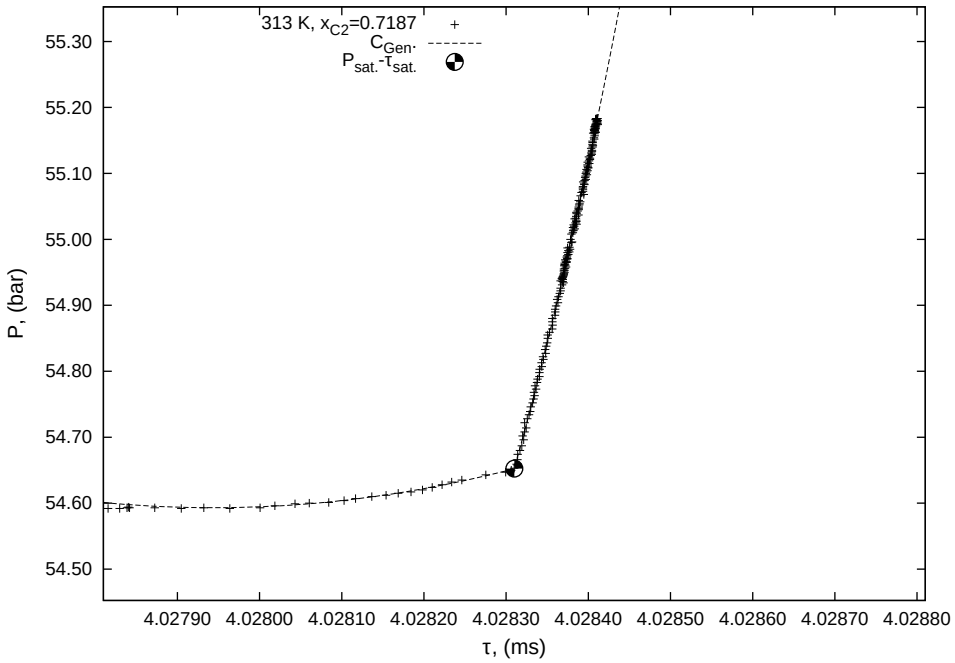

Figure 2: Detection of a L_H-G transition, x_{C_2} =0.7187, 314.15 K

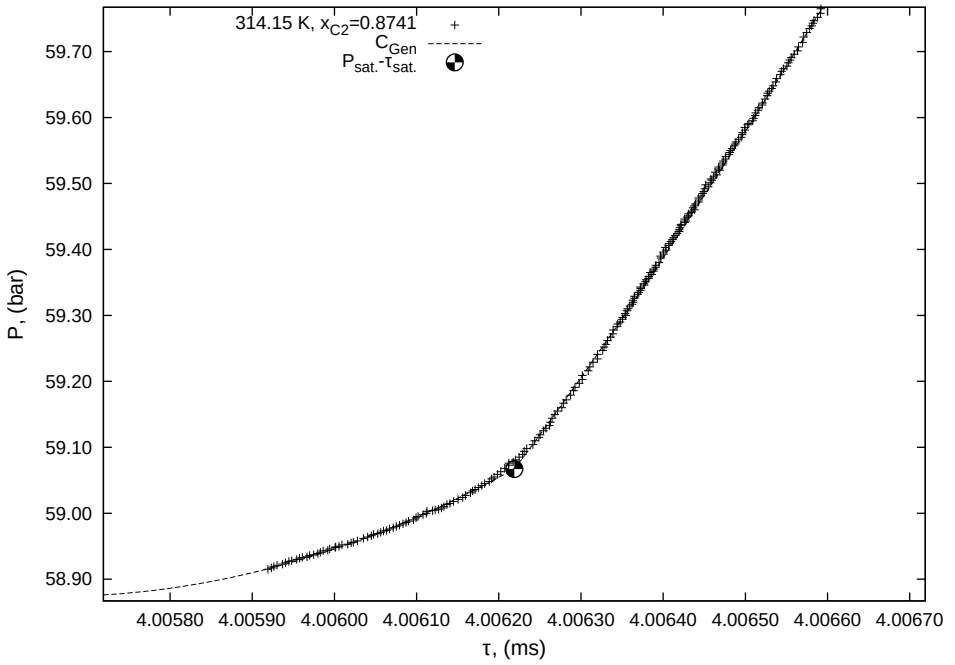

Figure 3: Detection of a L_L-L_H transition, x_{C_2} =0.8741, 314.15 K

Due to the slow migration of liquid drops of one liquid into the other, it can be assumed that the global composition of the fluid within the tube is relatively constant in a certain amount of time while the pressure is still lowering. It can be seen, for instance from the analysis of the data of Kodama et al. (2001), that the slope of ρ against p at constant composition and temperature must be positive within the inhomogeneous region and of an order of 7 $kg\,m^{-3}\,bar^{-1}$. This is of the same order of magnitude as the slope of ρ against x_{C2} at constant pressure for this fluid: 7 $kg\,m^{-3}\,(x\%)^{-1}$. The reason why the transition operates in the same direction as in the case of the

L_H – L_L in the $p - \tau$ or $p - \rho$ diagram is that, even if the local density of the heavy liquid in the mixture tends to increase when the L_L – L_H transition has initiated, the decrease of the bulk density of the inhomogeneous phase with the decreasing pressure is predominant. The composition must be relatively constant or vary much slowly than the pressure; the fluid is nearly following a tie line. It is what was detected by the vibrating tube. It is noticeable that the slope of the transition in figure 3 is higher than in figures 1 or 2. This can be explained by some competition between the two mentioned variations.

Figure 3 presents a topology similar to that of a liquid – gas transition, i.e. when the mixture is near critical. The only difference with this case is that the portion corresponding to the homogeneous phase in figure 3 is typical of a relatively incompressible liquid and not of a highly compressible near critical fluid (for which the curvature would be noticeably more pronounced).

3.2 Breakpoint determination

To determine the location of the breakpoint for each isotherm, values of $\tau_{BP} \simeq \tau_{Sat.}$ and $p_{BP} \simeq p_{Sat.}$ are estimated graphically from the collected data sets. Two additional data points are selected within the data set in the homogeneous region; one at about 1 or 2 bar above the estimated breakpoint: $\tau_{H,max}$, $p_{H,max.}$, and another one close to the breakpoint: $\tau_{H,min}$, $p_{H,min.}$. In the inhomogeneous region, a fourth data point; $\tau_{In,min.}$, $p_{In,min.}$ is selected that will set the extent of the considered inhomogeneous phase portion of the current isotherm.

Two curves are then defined to represent each portion of the isotherm. One stands for the homogeneous portion:

$$p_1(\tau) = p_{H,min.} + \sum_{k=1}^{k=p.d.H.} a_k(\tau - \tau_{H,min})^k$$

where $p.d.H.$ is a suitable polynomial degree for the current isotherm. Usually, $2 \leq p.d.H. \leq 4$ depending on the curvature of the isotherm and on the extent of the considered homogeneous region defined by the difference between $p_{H,max.}$ and $p_{H,min.}$. Another curve is set for the inhomogeneous portion of the isotherm:

$$p_2(\tau) = p_{In,min.} + \sum_{k=1}^{k=p.d.In.} b_k(\tau - \tau_{In,min})^k$$

where $p.d.In.$ =1 or 2 depending on the topology of the phase transition region. There is no reason to select higher polynomial degrees in this region.

In a first step, the two previous curves are fitted to the data in their respective region: from τ_{BP}, p_{BP} to $\tau_{H,max.}, p_{H,max.}$ for $p_1(\tau)$ and from $\tau_{In,min.}, p_{In,min.}$ to τ_{BP}, p_{BP} for $p_2(\tau)$. Once p_1 and p_2 are set they usually intersects near the stated τ_{BP}, p_{BP} but not necessarily within the experimental data set where the real breakpoint should be encountered. A continuous by parts curve is then build from the two previous that presents a jump a the searched coordinates of the breakpoint: τ^*_{BP}, p^*_{BP}. The corresponding function is defined as follows:

$$\hat{p}(\tau) = p_1(\tau)\sigma^+(\tau, \tau^*_{BP}) + p_2(\tau)\sigma^-(\tau, \tau^*_{BP})$$

where

$$\sigma^{\pm}(\tau, \tau^*_{BP}) = \frac{1}{1 + E\left(\pm 10^7 \left[\tau - \tau^*_{BP}\right]\right)}$$

and E is a *numerically safe* exponential:

$$\forall x \in \mathbb{R}, \quad E(x) = \begin{cases} \exp(x) \;\; if \;\; x \leq 10^2 \\ 10^{60} \;\; if \;\; x > 10^2 \end{cases}$$

This function can be fitted to the experimental data points in a limited range of τ around the estimated breakpoint period from $\tau_{In,min.} + (\tau_{BP} - \tau_{In,min.}/2)$ to $\tau_{H,min.}$, considering τ^*_{BP} as a new parameter to be determined. The function $\sigma^{\pm}(-)$ provides a sharp, near continuous jump centered on τ^*_{BP} with a bandwidth of about one tenth of the magnitude of the experimental fluctuations of τ. This jump is allowed to adjust to the data set during the fitting procedure providing a breakpoint that is located well within the bulk of experimental data. The fitting procedure provides the value of τ^*_{BP} and the pressure at this point is obtained from $\hat{p}(\tau^*_{BP})$.

This kind of automatic *breakpoint – tracking* procedure works well when the estimated location of this point can be obtained graphically with a good precision. To obtain the corresponding density at the breakpoint, the standard data treatment for the FPMC model is used (see Bouchot and Richon (2001)) with the data $\tau^*_{BP}, \hat{p}^*_{BP}, T$ as a pseudo – experimental data point. The uncertainties in the breakpoint coordinates are considered the same as on any other experimental data point at stable state conditions.

3.3 Topology of isotherms near the breakpoint

The topology of the different types of phase transitions encountered in the studied system is analyzed through a series of figures that show, at each nominal composition, a graph centered on the detected saturation point. In the following figures, the scale intervals on the period of vibration τ and on pressure p is the same for all; only the absolute values differ. The scale of τ is build around the saturation period $\pm 5 \times 10^{-4}$ ms and the scale of p is build around the saturation pressure -0.2 bar from the bottom of the figures and $+0.7$ bar to the top. The curves, C_{Gen}, on the figures correspond to the general correlations of the data, i.e. the graph of $\hat{p}(\tau)$. The points labeled as $P_{sat.} - \tau_{sat.}$ are the calculated breakpoints at coordinates $(\tau^*_{BP}, \hat{p}^*_{BP}, T)$.

These figures show various interesting features of the evolution of the fluid state as a function of pressure and composition. In what concerns the behavior of the homogeneous phases, it can be seen, thanks to the common scale intervals, how the slopes change depending on what fluid is present within the tube. For instance, the high slopes in figures 4 and 5 denote the presence of a heavy liquid and a sharp transition to a gas phase. In figures 6 and 7 the compressibility of the heavy liquid increases and the transition is smoother, from a heavy liquid to a light liquid or to a dense gas phase, depending on the temperature. These liquids are probably saturating at a pressure slightly higher than that of the three phase line.

In figures 8, 9 and 10, 11 the homogeneous phase behavior is similar, because both fluids are approaching the liquid – liquid critical point at slightly different compositions. The phase transitions are slightly different because the first two ones stand for a L_H – L_L (or dense gas) transition and in the next two ones for a L_L (or dense gas) – L_H transition.

The last two figures 12 and 13 are surprising at first sight because, while the temperature increases, the compressibility of the fluid seems to increase. The reason for this is that this fluid spans at least two types of transitions.

Breakpoints at $x_{C_2} \approx 71\%$

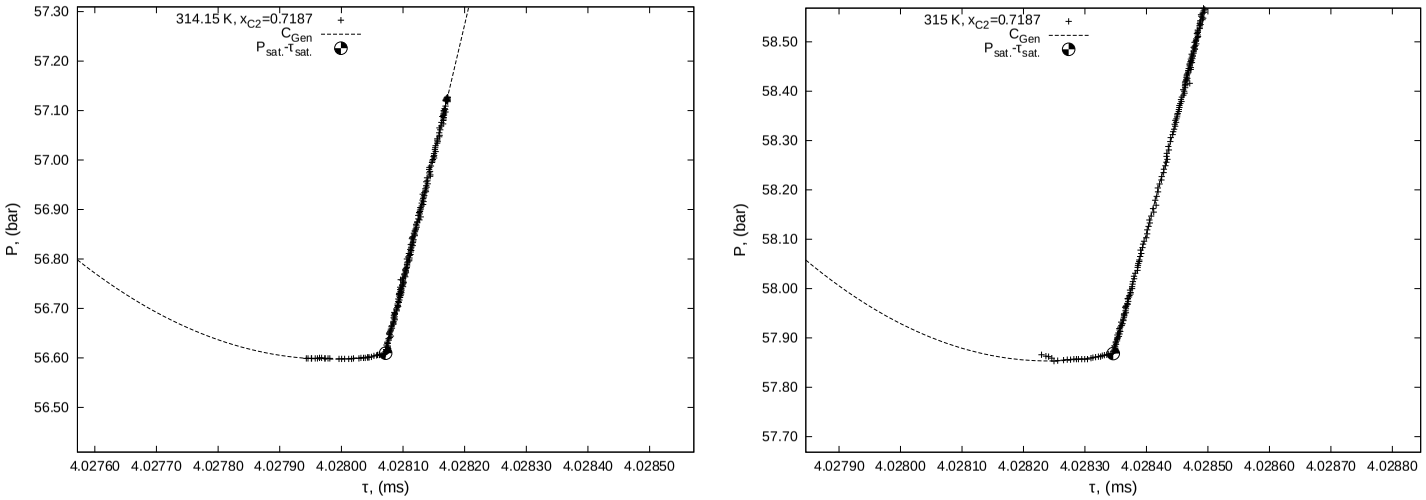

Figure 4: L_H – G transition at 314.15 K and 315 K

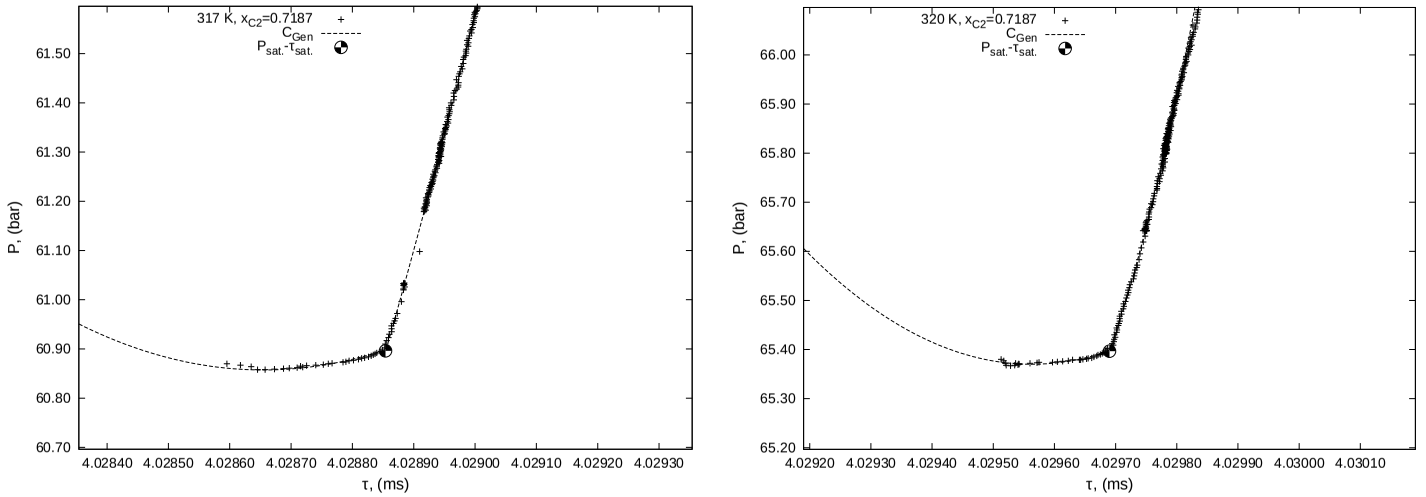

Figure 5: L_H – G transition at 317 K and 320 K

Breakpoints at $x_{C_2} \approx 83\%$

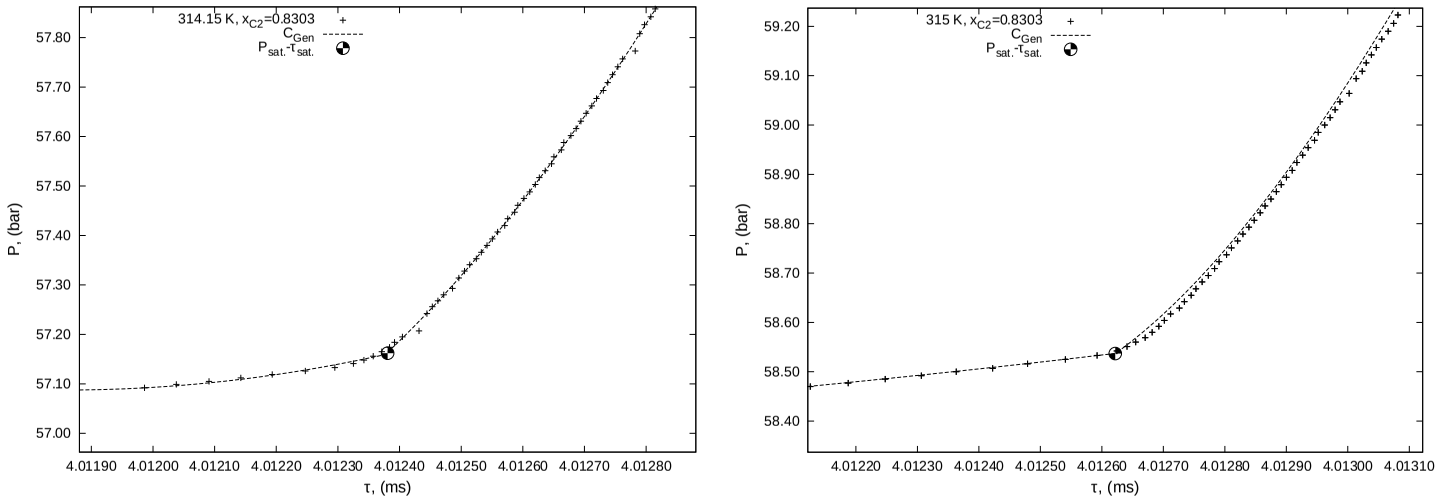

Figure 6: L_H – L_L transition at 314.15 K and 315 K

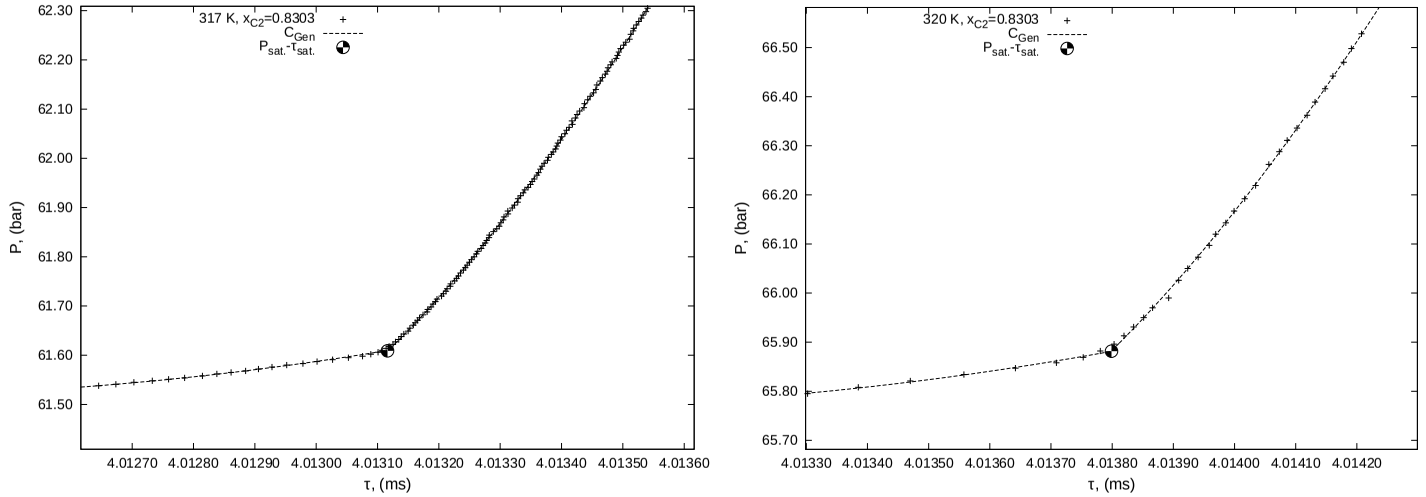

Figure 7: L_H – G transition at 317 K and 320 K

Breakpoints at $\mathbf{x}_{C_2} \approx 85\%$

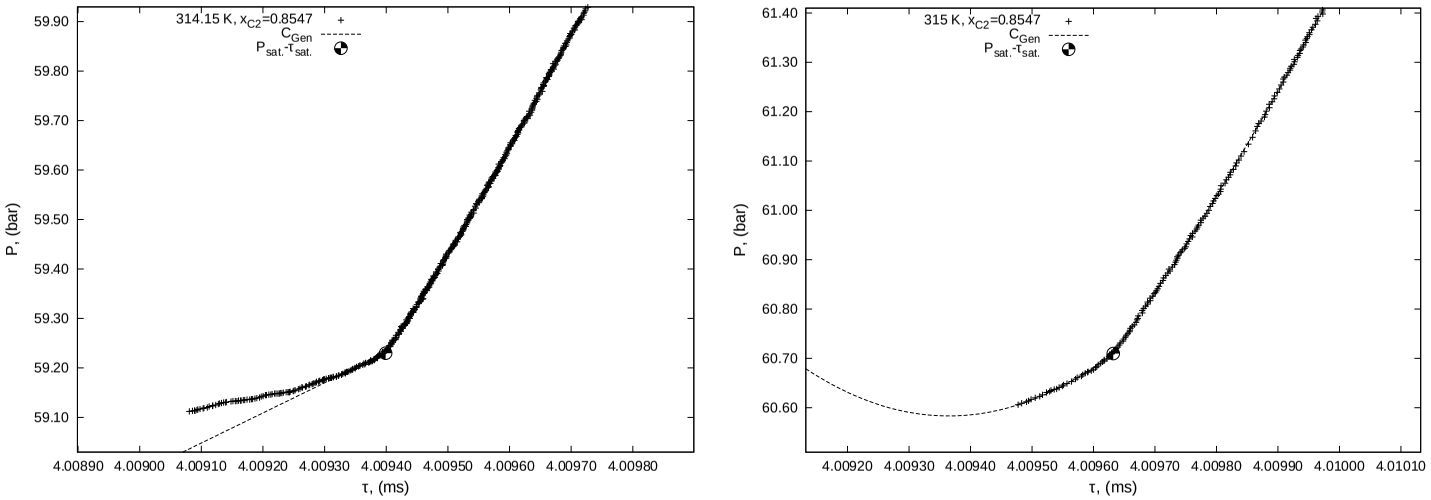

Figure 8: L_H – L_L transition at 314.15 K and 315 K

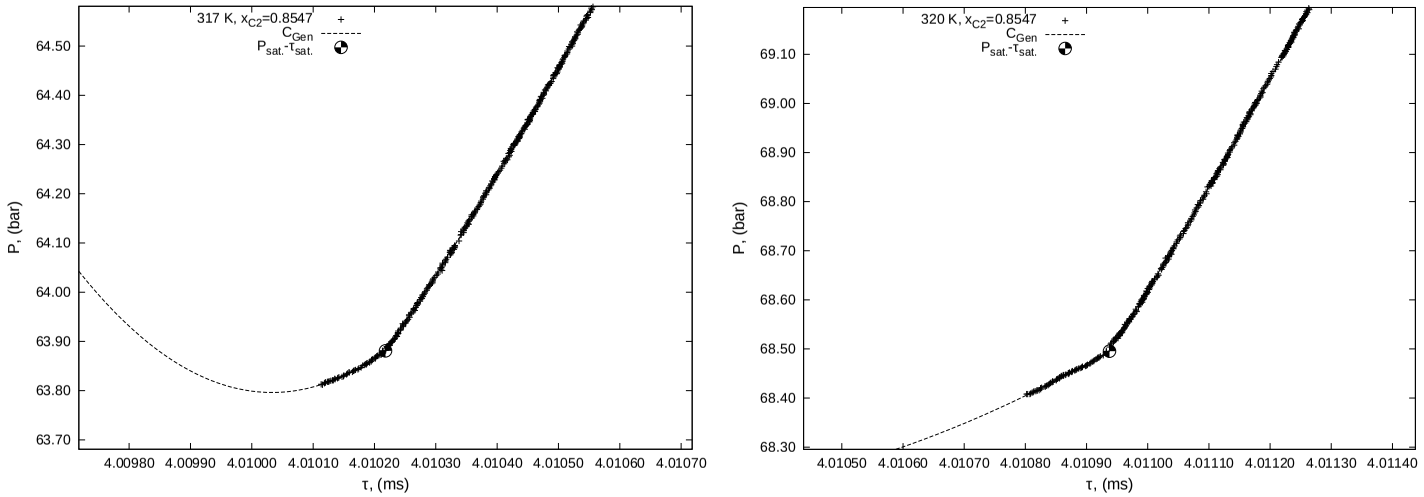

Figure 9: L_H – G transition at 317 K and 320 K

Breakpoints at $x_{C_2} \approx 87.5\%$

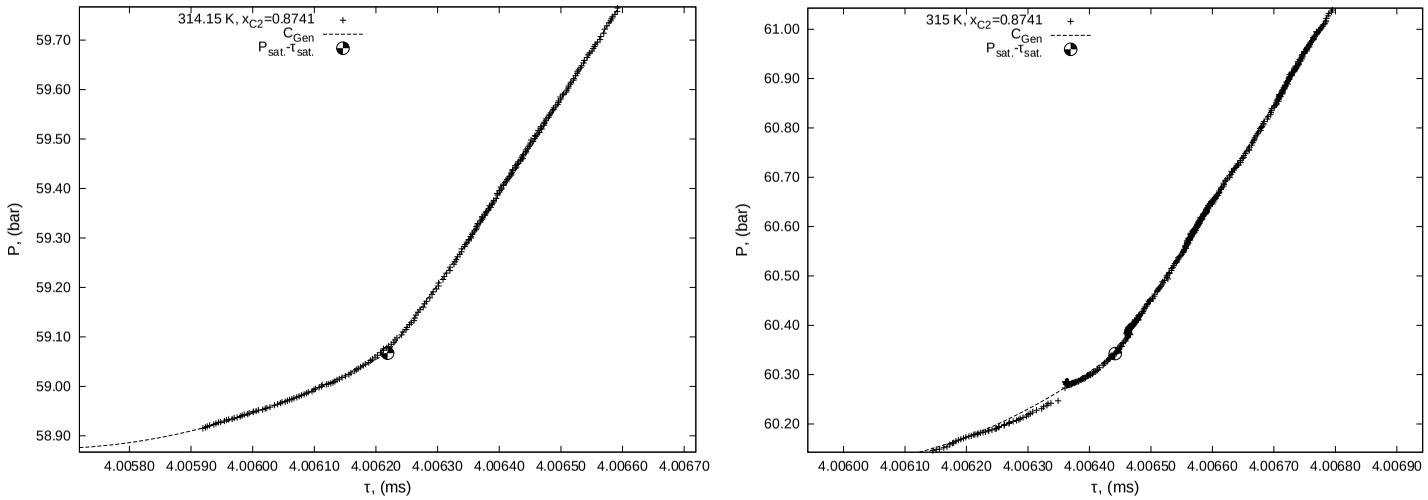

Figure 10: L_L – L_H transition at 314.15 K and 315 K

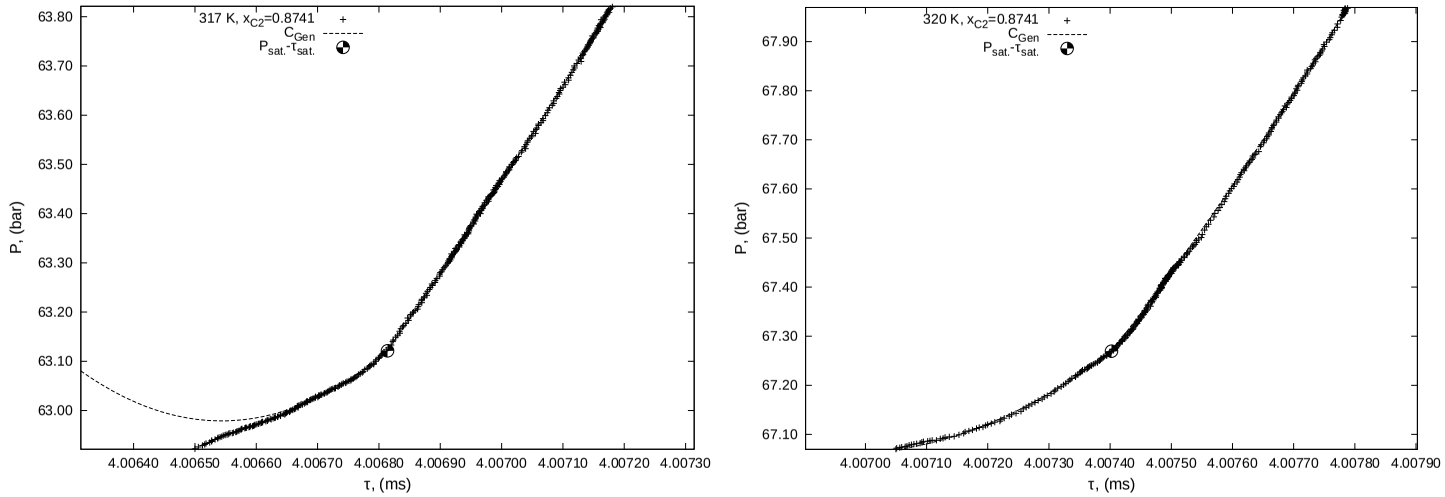

Figure 11: G – L_H transition at 317 K and 320 K

Breakpoints at $x_{C_2} \approx 90\%$

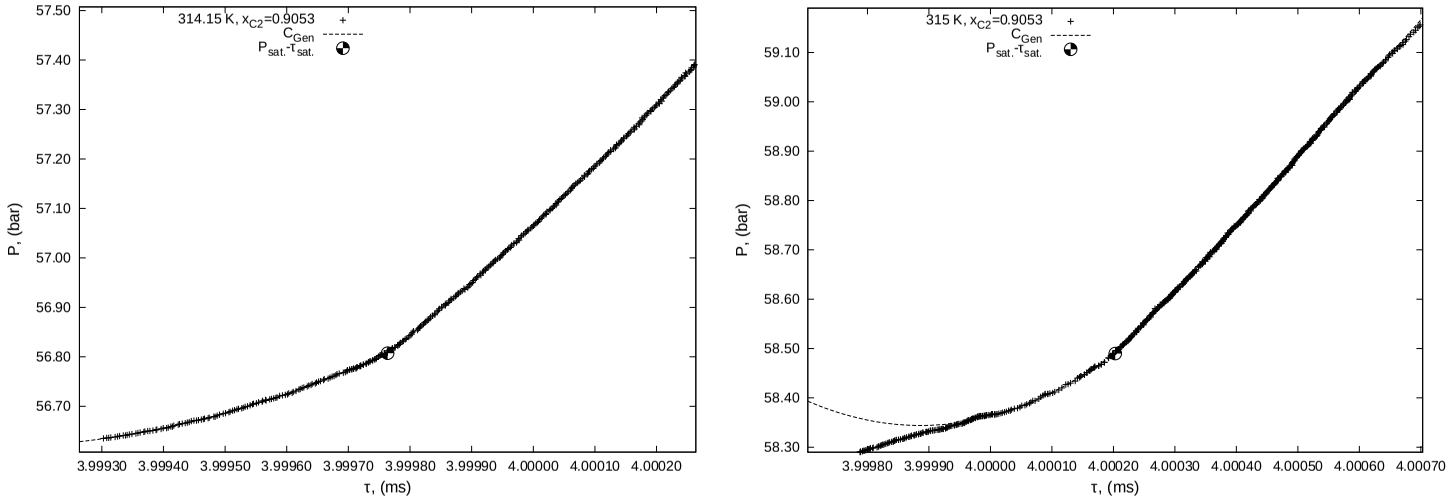

Figure 12: L_L – G transition at 314.15 K and L_L – (L_H - G) at 315 K

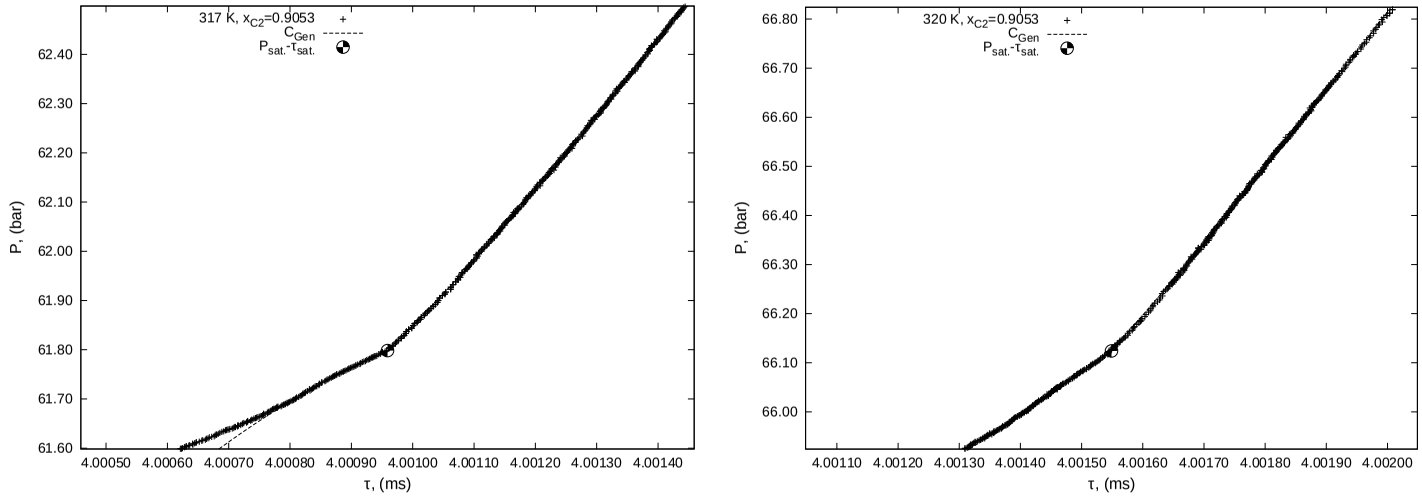

Figure 13: G – L_H transition at 317 K and 320 K

At 314.15 K the fluid presents a L_L – G transition in a state approaching the LG critical point of the mixture in the vicinity of the critical point of Ethane. This explains high slopes and a smooth transition due to the apparition of a gas phase in the light liquid. At 315 K, according to the data of Lam et al. (1990), the quantity of light liquid in the mixture is higher and the transition occurs near the three phase line. The liquid phase is denser, less compressible and the transition shows a less defined behavior that suggests that there is here a competition between the apparition of a dense liquid phase along with a gas phase in the light liquid bulk phase. At 317 K and 320 K, the type of transition has changed to a *liquid like* dense gas – L_H one, similar to what occurs in figures 10 and 11 but with a less dense fluid. The fact that the fluid at 320 K seems to be less compressible than at 317 K may indicate that this fluid is moving away from the L_H – G critical point and that the critical composition of the mixture with respect to Ethane is decreasing while temperature increases in this region (no critical compositions are reported in the literature).

3.4 A brief data comparison

The only available pvT – x data for the high pressure equilibrium behavior of the considered mixture are the data published by Kodama et al. (2001). These data are reported at 314.15 K and at pressures near the three phase line of the mixture.

Figures 14 and 15 present the data of this work in the p–x and ρ–x plane. Empirical smoothing functions are displayed to indicate the tendencies. The densities were obtained as indicated above in the text from the conversion of the periods.

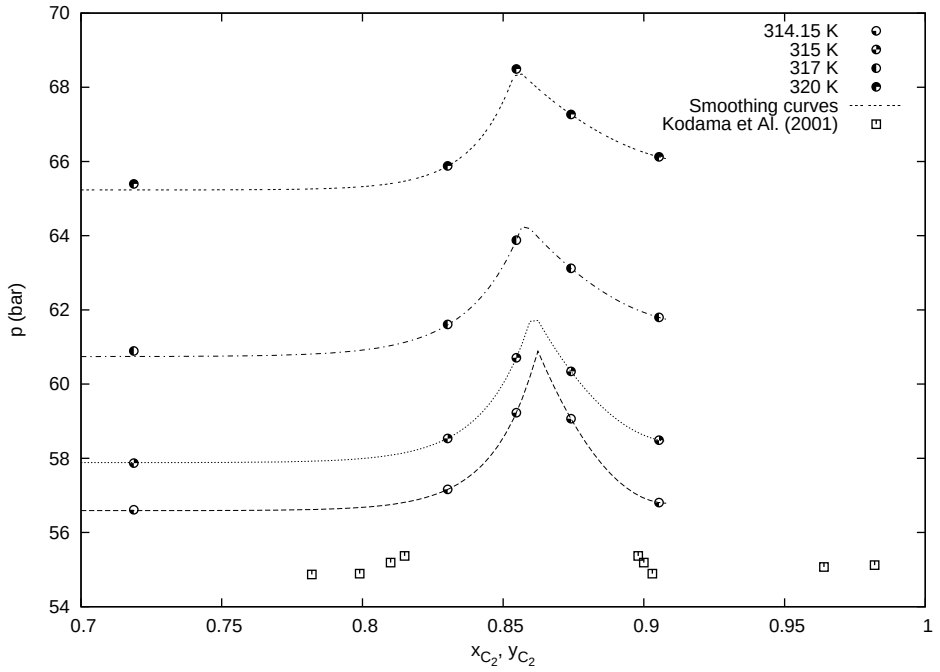

Figure 14: P –x,(x)y diagram for the Ethane + n-Propan-ol mixture

The evolution of our data with temperature shows a very good internal consistency in the p–x diagram, and the behavior of the four isotherm in the ρ – x plane is conform to what can be expected for this kind of mixtures. A rather high slope of ρ with respect to T at constant composition and the LL binodal with a low curvature in the ρ –x plane which can hardly be distinguished from the LG binodal. The LLE densities reported by Kodama et al. (2001) in the LL region span a clearly

larger plait in the ρ–x plane. As far as these densities correspond to pressures close to the three phase line, it can be assumed that as the composition will go closer to the LL critical point the densities would increase further.

There is a good consistency, in terms of compositions, between our data and those of Kodama et al. (2001) for the location of the opening of the LL in-miscibility window. However, the pressures measured in this work, are about 2 bar above those reported by the authors at 314.15 K. An estimation of the location of the LL and LG critical points from these two set of data show that there is also a total inconsistency of any of them with respect to the critical pressures reported by Brunner (1985); they are systematically higher. A dramatic influence of the purity of the fluids employed can be suspected and this point should be studied further.

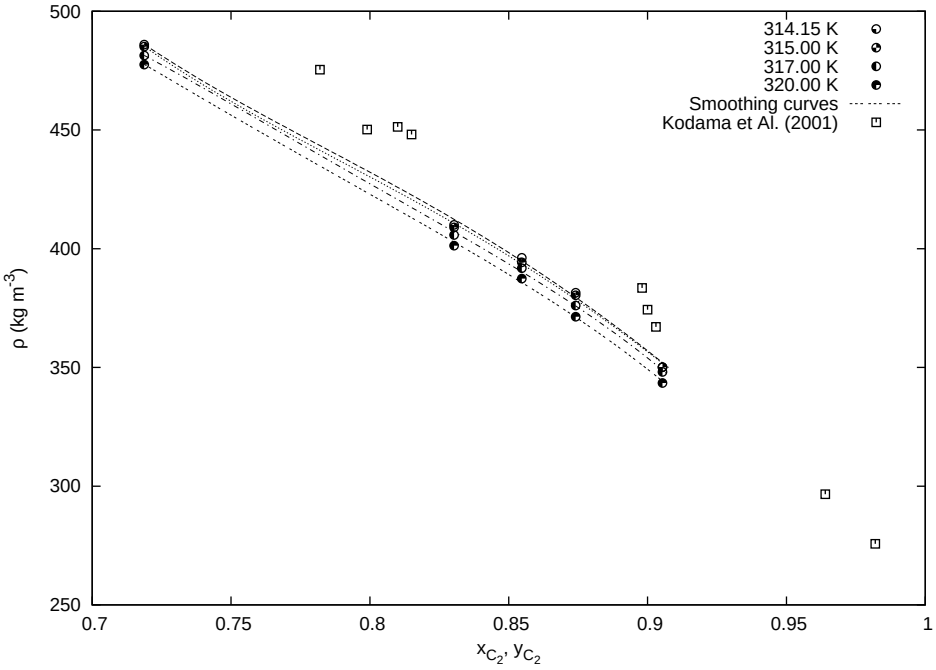

Figure 15: ρ –x,(x)y diagram for the Ethane + n-Propan-ol mixture

4 Conclusions

The phase transition behavior of a *Type V* binary mixture of Ethane + n-Propan-ol in a region where the fluid presents liquid – liquid transitions could be explored. This was performed using a setup including a single vibrating tube densitometer along with the appropriate methodology and procedures.

The breakpoints in the $p - \tau$ diagrams can be detected with good resolution and accuracy (basically the same as in the case of a L – V transition), and the information of the equilibrium pressure and of the density at saturation can be obtained straightfully from the standard data treatment for this particular technique. The topology of the transitions is clearly dependent of the nature of the involved phases. It can be explained by means of phenomenological arguments from the phase diagram of a particular fluid mixture and considerations about the functioning of the vibrating tube densitometer.

The technique proves to be efficient for this kind of measurements, even if the first data comparisons suggest that, for the particular case of the mixture Ethane + n-Propan-ol, the measured

data should be validated with another method and the same fluids. To our knowledge, these measurements are the first that have been obtained in this way at this time.

5 Acknowledgment

The authors are grateful to the Instituto Politécnico Nacional of México for financial support through the projects *CGPI 20030721/20040455*.

References

C. Bouchot and D. Richon. Direct pressure-volume-temperature and vapor-liquid equilibrium measurements with a single equipment using a vibrating tube densimeter up to 393 K and 40 MPa; description of the original apparatus and new data. *Ind. Eng. Chem. Res.*, 37:3295–3304, 1998a.

C. Bouchot and D. Richon. Vapor-liquid equilibria and densities of a chlorodifluoromethane (R 22) +1−chloro-1,2,2,2,-tetrafluroethane (R 124)+ 1-chloro-1, 1-difluoroethane (R 142b) mixture (R 409A) at temperatures between 253 K and 333 K and pressures up to 15.5 MPa (8010 data points). *International Electronic Journal of Physico-Chemical Data*, 4:89–98, 1998b.

C. Bouchot and D. Richon. An enhanced method to calibrate vibrating tube densimeters. *Fluid Phase Equilibria*, 191:189–208, 2001.

E. Brunner. Fluid mixtures at high pressures II. Phase separation and critical phenomena of (ethane + an n-alkanol) and of (ehtene + methanol) and (propane + methanol). *J. Chem. Thermodynamics*, 17:871–885, 1985.

J. De la Cruz de Dios, C. Bouchot, and L. A. Galicia Luna. New p-ρ-t measurements up to 70 MPa for the system CO_2+propane between 298 and 343 K at near crítical compositions. *Fluid Phase Equilibria*, 210:175–197, 2003.

L. A. Galicia Luna, D. Richon, and H. Renon. New loading technique for a vibrating tube densimeter and measurements of liquid densities up to 39.5 MPa for binary and ternary mixtures of the Carbon Dioxide - Methanol - Propane system. *J. Chem. Eng. Data*, 39:424–431, 1994.

C. D. Holcomb and S. L. Outcalt. A theoretically-based calibration and evaluation procedure for vibrating tubes densimeters. *Fluid Phase Equilibria*, 150-151:815–827, 1998.

D. Kodama, H. Tanaka, and M. Kato. High presure phase equilibrium for ethane + 1-propanol at 314.15 K. *J. Chem. Eng. Data*, 46:1280–1282, 2001.

B. Lagourette, C. Boned, H. Saint-Guirons, P. Xans, and H. Zhou. Densimeter calibration method versus temperature and pressure. *Meas. Sci. Technol.*, 3:699–703, 1992.

D. H. Lam, A. Jangkamolkulchai, and K. D. Luks. Liquid – liquid – vapor phase equilibrium behavior of certain binary ethane + n-alkanol mixtures. *Fluid Phase Equilibria*, 59:263–277, 1990.

Johanna Levelt Sengers. *How Fluids Unmix. Discoveries by the School of Van der Waals and Kamerlingh Onnes*. Royal Netherlands Academy of Arts and Sciences, 2002.